COMPTON SCATTERED IMAGING BASED ON THE V-LINE RADON TRANSFORM AND ITS MEDICAL IMAGING APPLICATIONS

M. K. Nguyen† *and R. Régnier*†

† Equipes Traitement de l'Information et Systèmes
CNRS 8051/ ENSEA / Université de Cergy-Pontoise
F-95302 Cergy-Pontoise Cedex, France

T. T. Truong[*] *and H. Zaidi*[‡] [*]

[*] Laboratoire de Physique Théorique et Modélisation
CNRS 8089/ Université de Cergy-Pontoise
F-95302 Cergy-Pontoise Cedex, France
[‡] Geneva University Hospital, Division of Nuclear Medicine
CH-1211 Geneva 4, Switzerland.

ABSTRACT

The Radon transform (RT) on straight lines deals as mathematical foundation for many tomographic modalities (*e.g.* X-ray scanner, Positron Emission Tomography), using only primary radiation. In this paper, we consider a new RT defined on a pair of half-lines forming a letter V, arising from the modeling a two-dimensional emission imaging process by Compton scattered gamma rays. We establish its analytic inverse, which is shown to support the feasibility of the reconstruction of a *two-dimensional* image from scattered radiation collected on a *one-dimensional* collimated camera. Moreover, a filtered back-projection inversion method is also constructed. Its main advantages are algorithmic efficiency and computational rapidity. We present numerical simulations to illustrate the working. To sum up, the V-line RT leads not only to a *new imaging principle*, but also to a *new concept of detector* with high energetic resolution capable to collect the scattered radiation.

Index Terms— Radon transforms, image reconstruction, nuclear imaging, tomography.

1. INTRODUCTION

Collecting first order Compton scattered radiation by a two-dimensional gamma camera from an object-medium for three-dimensional imaging purposes [1, 2] has turned out to be a recent attractive alternative to conventional tomographic emission imaging, which uses only primary (or non-scattered) radiation. This new imaging principle is modeled by the so-called Conical Radon Transform (CRT) and has been supported by numerical simulations [2]. Later on, extensions of this idea have been proposed in various directions [3]. In this paper, we describe the implementation of this idea for a one-dimensional gamma camera, which leads to a two-dimensional version of the CRT, called V-line Radon transform. The related imaging process may be realized, for example, on two-dimensional structures in biomedical imaging. Ideally, one can think of a radiation emitting flat object (or slice), in which Compton scattered radiation is collected by a collimated linear detector and used to reconstruct the primary radiation source distribution of this object (see Fig. 1).

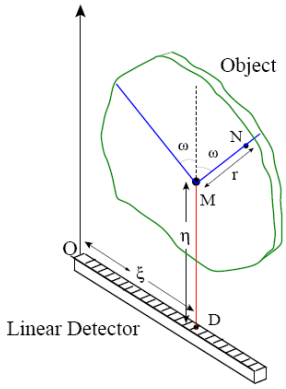

Fig. 1. Experimental setup and parameters used.

Section 2 shows how the image formation process by emission Compton scattered radiation is modeled and how the collected data by a linear collimated detector leads to a Radon transform on a pair of half-lines forming a letter V. This new integral transform, along with the conical Radon transform [1, 2, 3, 4], which we introduced a few years ago, is a novel class of Radon transforms, known in tomographic imaging. We establish its analytical inverse and derive a corresponding filtered back-projection. This last form has the advantage of reconstructing the image by fast algorithms. In section 3, we present numerical simulations on image reconstruction for a thyroid and a Shepp-Logan phantoms to support the feasibility of this imaging process. The paper ends with a short conclusion on the obtained results and opens some future research perspectives.

[*]Swiss National Science Foundation under grant No. 31003A-125246.

2. THE V-LINE RADON TRANSFORMATION

2.1. Image formation and the V-line Radon transform

Consider a 2D-object containing a non-uniform radioactivity source distribution, represented by a non-negative continuous function $f(x, y)$ with bounded support in $\{\mathbb{R}^2 | y > 0\}$. A collimated linear detector is set parallel to the plane of the object. It collects only outgoing radiation from the object which is parallel to the direction of the collimator holes (see Fig. 1).

If the detector is set to absorb gamma photons at energies below the energy of primary photons emitted by the object, the photons have undergone a Compton scattering at a site $\mathbf{M}$ in the bulk of the object under a scattering angle ω. Higher order scattering is neglected since it occurs with a much smaller probability. The photon flux density at a detecting site $\mathbf{D}$ is due to the sum of the contribution of all emitting object point sources located on two half-lines starting at a site $\mathbf{M}$ and making an angle ω with the collimator axis direction, for all possible $\mathbf{M}$ along the axis of the collimator at $\mathbf{D}$.

Let $f(x, y)$ be an activity density function, $\widehat{f}(\xi, \omega)$ the measured photon flux density at $\mathbf{D}$ under a scattering angle ω. Computing the photon flux density with the two-dimensional photometric law in the absence of radiation attenuation and for constant electronic density n_e, we can express $\widehat{f}(\xi, \omega)$ as

$$\widehat{f}(\xi, \omega) = K(\omega) \int_0^\infty \frac{d\eta}{\eta}\, T\mathbb{V}\, f(\xi, \eta, \omega), \tag{1}$$

where $K(\omega) = n_e\, P(\omega)$, $P(\omega)$ differential Compton scattering cross-section (Klein-Nishina formula [6]). This formula show that $\widehat{f}(\xi, \omega)$ is compounded of simpler integral transforms $T\mathbb{V}\, f(\xi, \eta, \omega)$ which may be written as

$$T\mathbb{V}\, f(\xi, \eta, \omega) = \int_0^\infty \frac{dr}{r}$$

$$\left[f(\xi + r\sin\omega, \eta + r\cos\omega) + f(\xi - r\sin\omega, \eta + r\cos\omega) \right]. \tag{2}$$

In the last integral, $f(x, y)$ is integrated on a discontinuous line having the form of a V-line with symmetry axis parallel to a fixed direction. Thus image formation by Compton scattered radiation in two dimensions leads to a new concept of a Radon transform on a V-line.

2.2. Definition

We now study the $T\mathbb{V}$ of equation (2) (η being constant). In particular for $\eta = 0$, this transform describes the imaging process of a one-dimensional collimated Compton camera, in which primary radiation emitted from the object bulk is scattered by a first linear scattering detector, lying along the Ox-axis of a cartesian coordinate system and collected by a second collimated absorbing detector.

For ease of notation we set $T\mathbb{V} f(\xi, \omega) = g(\xi, \omega)$ and observe that, because of the assumption on the support of f, the integral of equation (2) is well-defined. ξ gives the position of the vertex on the Ox axis. The factor $1/r$ in the integrand accounts for the photometric law of photon propagation in two dimensions. As $K(\omega)$ is a known factor, it shall be ignored to concentrate on the essential. Under the change of variables $t = \tan\omega$ and $z = r\cos\omega$, equation (2) reads

$$g(\xi, \omega) = G(\xi, t) = \int_0^\infty \frac{dz}{z} \left[f(\xi + tz, z) + f(\xi - tz, z) \right]. \tag{3}$$

2.3. The inverse transform $T\mathbb{V}^{-1}$

The inverse transform $T\mathbb{V}^{-1}$ can be worked out using Fourier transforms $\widetilde{f}(q, y)$ (resp. $\widetilde{g}(q, \omega)$) with respect to the variable x (resp. ξ) in $f(x, y)$ (resp. $g(\xi, \omega)$)), *i.e.*

$$(g(\xi, \omega), f(x, y)) = \int_{-\infty}^\infty dq\ (\widetilde{g}(q, \omega)\, \widetilde{f}(q, y))\ \exp(2i\pi q\xi). \tag{4}$$

Then equation (3) becomes

$$\widetilde{g}(q, \omega) = \int_0^\infty \frac{dz}{z}\, \widetilde{f}(q, z)\, 2\cos(2\pi q\, z\, t). \tag{5}$$

Defining $\widetilde{G}(q, t) = \widetilde{g}(q, \omega)$ with $\widetilde{F}(q, z) = \widetilde{f}(q, z)/z$, equation (3) appears as a cosine-Fourier transform

$$\widetilde{G}(q, t) = \int_0^\infty dz\ \widetilde{F}(q, z)\ 2\cos(2\pi q z t). \tag{6}$$

Thus the inverse formula reads in Fourier space

$$\widetilde{F}(q, z) = 2|q| \int_0^\infty dt\ \cos(2\pi q t z)\ \widetilde{G}(q, t). \tag{7}$$

2.4. Filtered back-projection inversion method (FBP-IM)

In this section we establish another formulation of the inversion procedure which lends itself more advantageous to algorithmic implementation. We call it *filtered back-projection* (FBP), due to its similarity to the one of standard Radon transform, but the novelty is that the FBP is carried on the V-lines but not on the straight lines. In the Radon transform the FBP is an exact inversion formula obtained by combining the action of the ramp filter and the back-projection operation of the Radon transform. In this section, we will demonstrate that the $T\mathbb{V}$ transform may be inverted essentially in the same way, the ramp filter and the back-projection operator associated to the $T\mathbb{V}$ operator playing an analogous role. Technically the back-projection principle consists in assigning the value $g(\xi, \omega)$ to every point on the "projection" V-line, which has given rise to this value, and then to sum over all contributions for every V-line "projection". More precisely, the back-projection at angle ω in (x, y) is the sum of projections

at angle ω at the points $\xi_1 = x+y\tan\omega$ and $\xi_2 = x-y\tan\omega$, where (x, y) is projected:

$$R_\omega(x,y) = g\left(x + y\tan\omega, \omega\right) + g\left(x - y\tan\omega, \omega\right). \quad (8)$$

The back-projection of every projection defines the back-projection operator $T\mathbb{V}^\#$ which is obtained by summing over every angle ω the expressions given in equation (8). Here a y-factor appears because of dr/r in the definition of the projections (2). Now the action of the ramp filter operator Λ over a function $f(x, y)$ in the first variable is defined in Fourier space by $\widetilde{\Lambda f}(q, y) = |q|\tilde{f}(q, y)$, where the Fourier transform is taken on x. From equation (7) we have

$$f(x,y) = y\int_0^\infty dt\left[(\Lambda g)(x+ty,t) + (\Lambda g)(x-ty,t)\right].$$

Setting $\mathcal{M}_\omega = g(\xi,\omega)/\cos 2\omega$ and using the expression of $T\mathbb{V}^\# g(x, y)$, we recover $f(x, y)$ by a filtered-back projection as $f(x,y) = y\left(T\mathbb{V}^\#\mathcal{M}_\omega\Lambda\, T\mathbb{V}f\right)(x,y)$.

3. NUMERICAL SIMULATIONS

We present now the results of numerical simulations. The original images (Figs. (2,5)) of size 512×512 of length units are respectively a thyroid with small nodules phantom and a Shepp-Logan phantom. Figs. (3,6) show the $T\mathbb{V}$ transform of the phantoms with angular sampling rate $d\omega = 0.005$ rad and 314 projections ($\pi/2/0.005 = 314$) which are the images of Compton scattered radiation on the camera in terms of the distance ξ and the scattering angle ω. The reconstructions using FBP are given in Figs. (4,7). The artifacts are due to the limited number of projections. Moreover, back-projection on V-lines generates more artifacts than back-projection on straight lines, because of more spurious line intersections (two V-lines have at most two intersections whereas two straight lines meet only at one intersection, the intersection which does not correspond to the true object pixel generates an artifact). A choice of a smaller $d\omega$ would improve image quality. For example with $d\omega = 0.005$ rad we have a Mean Square Error (MSE) of 2.8×10^{-3} whereas with $d\omega = 0.0025$ rad the MSE is 2.0×10^{-3}. It is observed that the small structures in the object are clearly reconstructed, in particular when the detector is placed near the object to collect much more scattered radiation. This result illustrates undoubtedly the feasibility of the new imaging modality, for which the main advantage resides in the use of a *one-dimensional non-moving* collimated Compton camera for *two-dimensional* image processing.

The main aim of this work is to establish a new imaging principle by Compton scattered radiation. This is why other factors in realistic imaging systems are not treated here such as medium attenuation, inhomogeneous electron density and Poisson emission noise.

4. CONCLUSION

In this paper, a new class of Radon transform defined on a discontinuous line, having the shape of a V letter is presented. We construct its analytic inverse transform as well as the corresponding filtered back-projection inversion method. They allow two-dimensional image reconstruction from scattered radiation collected by a one-dimensional collimated camera. We have also performed numerical simulations to prove its practical viability. This new scattered radiation imaging provides an alternative to existing primary radiation imaging. On the other hand, the results obtained for the TV with fixed axis direction is a necessary step to tackle the case of the swinging axis V-line Radon transform for a two-dimensional Compton camera imaging, as proposed by Basko *et.al.* [5]. Furthermore, the extension of this transform to a family of cones with swinging axis around a site in $\mathbb{R}^3$, for a concrete gamma camera without mechanical collimator, poses a real mathematical challenge to overcome in the future. Moreover this new imaging may have applications beyond the medical field in homeland security and in non-destructive industrial testing.

5. REFERENCES

[1] Nguyen M K and Truong T T, On an integral transform and its inverse in nuclear imaging *Inverse Problems* vol. 18, pp. 265-277, 2002.

[2] Nguyen M K, Truong T T, Bui H D and Delarbre J L, A novel inverse problem in γ-rays emission imaging *Inverse Problems in Science and in Engineering*, vol. 12, pp. 225-246, 2004.

[3] M. K. Nguyen, T. T. Truong, C. Driol and H. Zaidi, *On a novel approach to Compton scattered emission imaging*, IEEE Transactions in Nuclear Sciences, vol. 56, pp. 1430-1437, 2009.

[4] T. T. Truong, M. K. Nguyen and H. Zaidi, The mathematical foundations of 3D Compton scatter emission imaging, *International Journal of Biomedical Imaging, Special Issue on Mathematics in Biomedical Imaging*, doi: 10. 1155/2007/92780, 2007.

[5] R. Basko, G.L. Zeng, G. T. Gullberg, Analytical reconstruction formula for the one-dimensional Compton camera, *IEEE Trans. Nucl. Sci.*, vol.44, pp. 1342-1346, 1997.

[6] Barrett H H, The Radon Transform and its Applications in *Progress in Optics*, vol. 21, pp. 219-286, Ed. E. Wolf, North Holland, 1984.

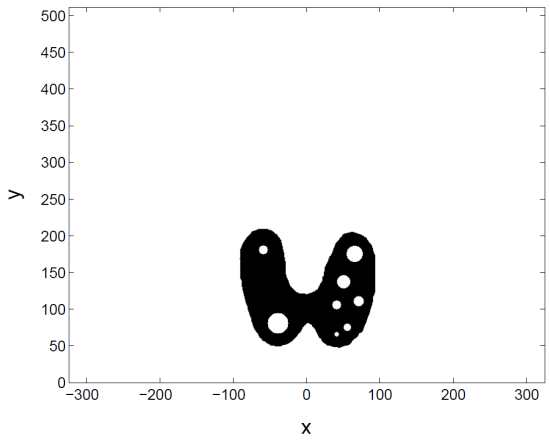

Fig. 2. Original thyroid phantom.

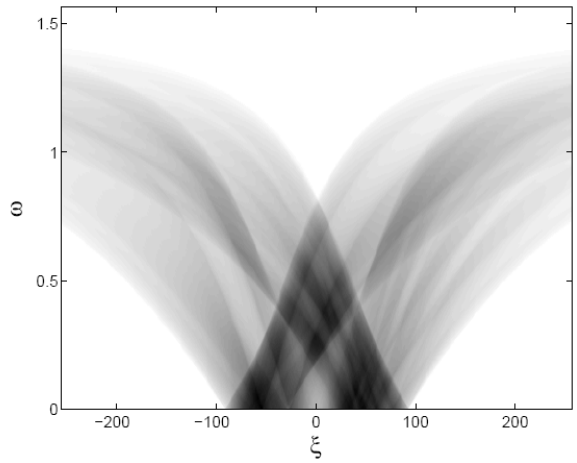

Fig. 3. The $T\mathbb{V}$ transform of the thyroid image shown in Figure 2 with $d\omega = 0.005$ rad.

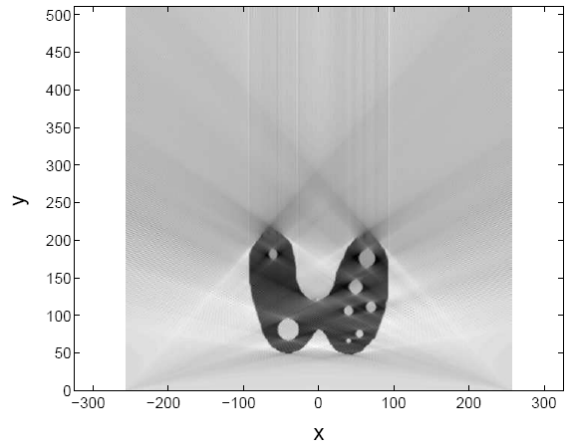

Fig. 4. FBP-IM reconstruction with ($d\omega = 0.005$ rad).

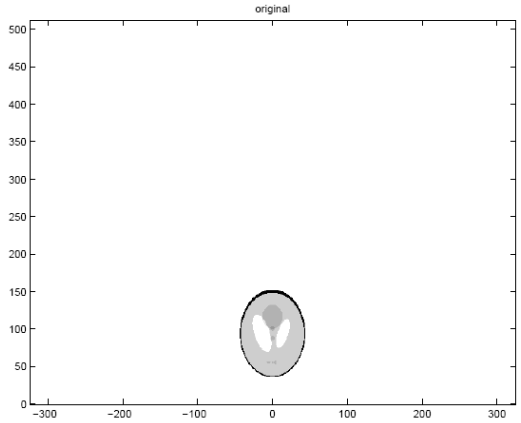

Fig. 5. Original Shepp-Logan phantom.

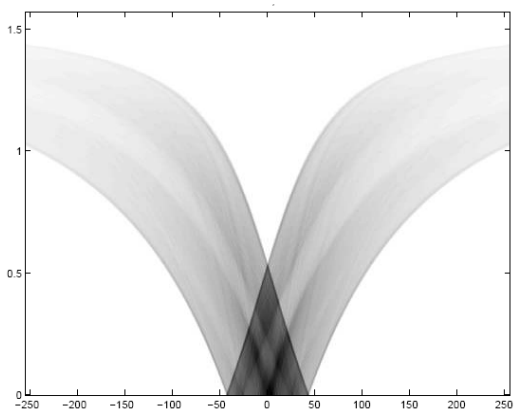

Fig. 6. The $T\mathbb{V}$ transform of the Shepp-Logan image shown in Figure 5 with $d\omega = 0.005$ rad.

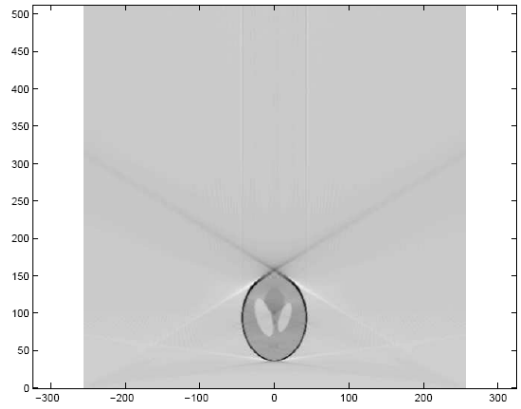

Fig. 7. FBP-IM reconstruction ($d\omega = 0.005$ rad).